

# Low-Magnitude High-Frequency Mechanical Signals Accelerate and Augment Endochondral Bone Repair: Preliminary Evidence of Efficacy

Allen E. Goodship,<sup>1,2</sup> Timothy J. Lawes,<sup>1,2</sup> Clinton T. Rubin<sup>3</sup>

<sup>1</sup>Royal Veterinary College, Hawkshead Lane, North Mymms, Hatfield, Hertfordshire, United Kingdom AL9 7TA, <sup>2</sup>University College London, Royal National Orthopaedic Hospital, Stanmore, Middlesex, United Kingdom, <sup>3</sup>Department of Biomedical Engineering, State University of New York at Stony Brook, Stony Brook, New York

Received 26 March 2008; accepted 30 October 2008

Published online in Wiley InterScience (www.interscience.wiley.com). DOI 10.1002/jor.20824

**ABSTRACT:** Fracture healing can be enhanced by load bearing, but the specific components of the mechanical environment which can augment or accelerate the process remain unknown. The ability of low-magnitude, high-frequency mechanical signals, anabolic in bone tissue, are evaluated here for their ability to influence fracture healing. The potential for short duration (17 min), extremely low-magnitude (25  $\mu\text{m}$ ), high-frequency (30 Hz) interfragmentary displacements to enhance fracture healing was evaluated in a mid-diaphyseal, 3-mm osteotomy of the sheep tibia. In a pilot study of proof of concept and clinical relevance, healing in osteotomies stabilized with rigid external fixation (Control:  $n = 4$ ), were compared to the healing status of osteotomies with the same stiffness of fixation, but supplemented with daily mechanical loading (Experimental:  $n = 4$ ). These 25- $\mu\text{m}$  displacements, induced by a ferroactive shape-memory alloy ("smart" material) incorporated into the body of the external fixator, were less than 1% of the 3-mm fracture gap, and less than 6% of the 0.45-mm displacement measured at the site during ambulation ( $p < 0.001$ ). At 10-weeks post-op, the callus in the Experimental group was 3.6-fold stiffer ( $p < 0.03$ ), 2.5-fold stronger ( $p = 0.05$ ), and 29% larger ( $p < 0.01$ ) than Controls. Bone mineral content was 52% greater in the Experimental group ( $p < 0.02$ ), with a 2.6-fold increase in bone mineral content (BMC) in the region of the periosteum ( $p < 0.001$ ). These data reinforce the critical role of mechanical factors in the enhancement of fracture healing, and emphasize that the signals need not be large to be influential and potentially clinically advantageous to the restoration of function. © 2008 Orthopaedic Research Society. Published by Wiley Periodicals, Inc. *J Orthop Res*

**Keywords:** fracture healing; mechanical; callus; loading; endochondral bone repair

Bone tissue has long been recognized as sensitive to mechanical loading, in a manner which can have either beneficial (anabolic) or destructive (catabolic) consequences. Extrapolating this adaptive capacity to the role of mechanical signals on bone healing, it should not be surprising that loading also has a critical influence on the repair of skeletal fractures,<sup>1,2</sup> either in enhancing the response,<sup>3,4</sup> or, in cases of too much loading, derailing the healing process.<sup>5,6</sup> While these "form follows function" rules of the skeleton, originally formulated by observing the morphologic patterns of healing bones and outlined in "Wolff's Law of Bone Remodeling,"<sup>7</sup> only very few guidelines exist which help define the ideal mechanical environment of healing tissue towards the restoration of biomechanical function.<sup>8</sup>

Bone healing is subject to mechanical signals, as regulated via stiffness of fixation, rigidity of cast immobilization, control of weight bearing, or even applied loading of the fracture site, can influence the quality, rate, and progression of repair.<sup>9,10</sup> For example, too much loading can compromise the healing response, as evidenced by a delayed union as exacerbated by early weight bearing on a fracture protected only by flexible external fixation.<sup>5</sup> While decreased frame stiffness stimulates periosteal callus, excessive motion is permissive to chondrogenesis, particularly where high levels of intermittent shear occurs,<sup>11,12</sup> and may lead to hypertrophic nonunion. Frames with low stiffness character-

istics may also result in high pin/bone interface stresses that induce local resorption and associated pin loosening.<sup>13</sup> At the other extreme, external fixation with high frame stiffness can suppress the osteogenic response at the periosteum, and is permissive to a delayed or atrophic nonunion,<sup>4,6</sup> while internal fracture fixation, via plates which are too stiff, can cause osteopenia below the device.<sup>14</sup>

The paradox between harnessing mechanical signals as beneficial to bone healing and avoiding those which damage the process further incites a challenge to identify a mechanical environment which is both safe and enhances the repair process. A strategy to establish the relevant window between compliant and rigid fixation has been approached by using external fixation with high rigidity except in the axial direction, and thus permitting passive, controlled loading of the fracture gap, or the external application of directed, dynamic axial interfragmentary motion.<sup>1</sup> Indirect fracture repair can be enhanced by applying axial cyclical interfragmentary motions with specific characteristics for short daily periods, without potentiating risk to the fracture gap which might arise during functional loading but poor protection afforded by low rigidity of the fixator.<sup>10,15–17</sup> While limited interfragmentary motion is accepted as anabolic to the healing response, it remains unclear if the potential benefits of loading in the laboratory setting can exceed the risks inherent in the clinic of overloading the repair site and thus promoting a pathologic response.<sup>18</sup>

The osteogenic potential of strain magnitude is well recognized,<sup>19</sup> but does not, in isolation, govern bone's response to mechanical loading. Other factors such as the number of loading cycles,<sup>20</sup> strain rate,<sup>21</sup> and spatial

Correspondence to: Allen E. Goodship (T: +44-208-909-5535; F: +44-208-954-8560; E-mail: goodship@rvc.ac.uk)

© 2008 Orthopaedic Research Society. Published by Wiley Periodicals, Inc.

strain gradient<sup>22</sup> also play a significant role in the osteogenic capacity of mechanical loading. It has been shown previously that extremely low magnitude (<10 microstrain), when induced at high frequencies (20–90 Hz) can be strongly anabolic to bone tissue.<sup>23</sup> Furthermore, these strain signals represent a central component of bone's strain history, and while not large, are omnipresent in the skeleton's functional regime.<sup>24</sup> Considering the low amplitude of these signals, it was postulated that they could be introduced to the fracture gap at levels well below those which cause risk to the regenerate tissue,<sup>25</sup> yet may promote the healing response. The study reported here tested the hypothesis that specific low-amplitude, high-frequency interfragmentary displacements will accelerate the process of bone healing.

## METHODS

### Fracture Model

All procedures were reviewed and approved by the UK regulatory authorities. Skeletally mature, female English mule cross sheep, 5–6 years of age were used for this study. Under general halothane anesthesia and post-operative analgesia, mid-diaphyseal 3-mm osteotomies of the tibia were created in two groups of four sheep and stabilized by unilateral stiff external fixation (1,100 N/mm axial stiffness), with anatomically standardized osteotomy and frame geometry. A low-energy osteotomy was performed using a Gigli wire with the osteotomy gap set with a spacer to 3 mm. Osteotomy and fixator geometry were standardized with intraoperative jigs which reproduced pin position, osteotomy site, fixator to bone offset, and interfragmentary gap. To accommodate the linearly variable differential transducers (LVDTs) for measuring interfragmentary displacement, accessory half pins were inserted 90° to the fixator frame pins using the same intraoperative jig which positioned the fixator and osteotomy. Interfragmentary motion during periods of stimulation were made possible in a rigid fixation system through the use of a shape-memory alloy (see below).

The Control group of sheep was permitted to heal over a 10-week postoperative period, with the fixator locked to retain frame stiffness throughout. The fixator used in the Experimental group was similarly locked from motion, with the addition of short, daily periods (17 min) of low-magnitude, high-frequency cyclical interfragmentary motion, in which a current driving a shape-memory alloy induced small displacements in the rigid fixator. The stimulus was applied 5 days per week (Fig. 1).

### Dynamic Fixator

A high-response, high-force magnetostrictive shape-memory actuator (Terfenol-D, Etrema Products, Ames, IA), made from terbium, dysprosium, and iron,<sup>26</sup> was incorporated as part of the fixator body, such that longitudinal displacement, in the absence of any "moving parts," would cause direct displacement of the osteotomy site. In contrast to piezoelectric crystals, such terbium-based shape-memory alloys can displace (extend/contract) very efficiently with low voltages, are strong, and are not brittle, thus allowing the fixator shaft to be comprised of the alloy without need for reinforcement. The response time of this material exceeds 5 KHz.

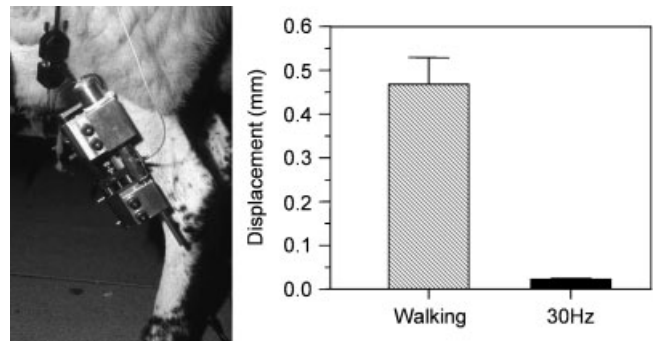


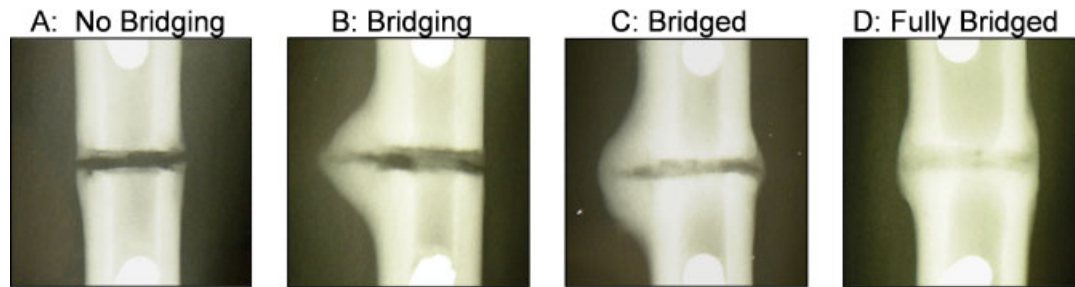
**Figure 1.** The application of the 30-Hz low-strain mechanical stimulus directly to the fracture site on the sheep tibia via an external fixator, the body of which is made from a shape memory alloy (left). Measured 1-week postoperatively, peak interfragmentary motion during walking (average of both groups  $\pm$  SD) was 20 $\times$  greater than the 25  $\mu$ m displacement caused by the 30-Hz stimulation of the fracture callus in the Experimental group.

Thirty Hertz (cycles per second), low-amplitude (25  $\mu$ m) sinusoidal interfragmentary motion was applied daily 5 days per week. Experimental animals were not anesthetized during the period of stimulation. For 17 min each day, both the Experimental and Control animals were confined to a small stall, and showed no signs of discomfort (e.g., movement, agitation) during this confinement and/or loading period. The same short period of 17 min was used as in prior mechanical stimulation of fracture repair studies performed on animals<sup>9</sup> and humans.<sup>10</sup>

Displacements of 25  $\mu$ m limited the imposed interfragmentary movement to approximately 0.8% of the overall 3-mm osteotomy gap and remained well below the ultimate strain of mature cortical bone of 2%.<sup>27</sup> Interfragmentary displacement was monitored each day using Linearly Variable Displacement Transducers (Sangamo Schlumberger UK gauging LVDTs, max displacement 10-mm resolution 2.5- $\mu$ m, current equivalent Solartron Metrology, Bognor Regis, West Sussex, UK); mounted on the nonload-bearing accessory half pins implanted directly into the cortical bone.<sup>15</sup> While the actuator was displacement controlled, current to the actuators was regulated such that the force generated to induce the displacements never exceeded 50 N, less than 10% of the animals weight, thus minimizing the risk of damaging the healing callus (i.e., forces generated by weight bearing exceeded that imparted by the actuator). While the displacements of the active actuator were defined at time of surgery, they were not monitored over the course of the study.

### Radiography

Radiographs of the developing callus were taken post-op and on a weekly basis, aided by an alignment jig coupled to the fixator pins to reproduce position and standardized exposure with an aluminium step wedge phantom. The maximum callus diameter was measured from the standard view radiographs using dial gauge callipers ( $\pm$ 0.01 mm) calibrated against a size phantom on each radiographic film, and blind assessments made of the quality of union. Each callus was scored as (a) no bridging, (b) some cortical bridging, (c) all cortices bridged, or (d) fully bridged cortices with loss of cortical

**Table 1.** Radiographic Assessment of Healing Fractures at Week 10<sup>a</sup>

Control	Radiographic Assessment	Callus Diameter (mm)
C1	(b) Bridging	17.1†
C2	(b) Bridging	20.5
C3	(b) Bridging	19.1
C4	(a) No bridging	22.3
Mean		19.9 ± 2.2
Experimental		
E1	(c) Bridged	26.8
E2	(c) Bridged	27.5
E3	(d) Fully bridged	21.8
E4	(c) Bridged	26.6
Mean		25.7 ± 2.6

<sup>a</sup>Performed both by subjective evaluation of healing status (visual reading of radiographs, performed without knowledge of Control/Experimental status, and assigned to one of four stages, from no bridging to fully bridged), and objective evaluation of callus diameter. (Magnification compensated with calibration standard on film; †cortical border used as callus diameter due to lack of callus.) At the top are representative radiographs of the four stages: (A) no bridging; (B) bridging; (C) bridged; (D) fully bridged. The callus size in Controls was 22.7% smaller than that measured in the Experimental animals ( $p < 0.01$ ).

definition, indicative of matrix remodeling and maturation (Table 1).

#### DEXA Bone Mineral Content

Using dual-energy X-ray absorptiometry (DXA; Hologic QDR 1000W, Vertec Scientific, Reading UK), bone mineral content (BMC) of the callus was measured at baseline and each week in three regions of interest (ROI), with realignment facilitated by a repositioning jig focused using the fixator pins. ROIs included the entire callus, which was then subdivided into the intramembranous bone formation budding from the osteogenic layer of the periosteum and endochondral formation in the interfracture gap (Fig. 2). The values of BMC at

1-week postoperatively were subtracted from each following scan to obtain the total new bone mineral in each ossification region.

#### Locomotor Analysis

Peak vertical ground reaction force (GRF) and simultaneous peak interfracture motion was measured weekly by walking the sheep across a force plate (Kistler Instruments, Hampshire, UK). Peak interfracture motion was measured with a three degree-of-freedom array of LVDTs (Sangamo Transducers, Sussex, UK) mounted on the nonload-bearing accessory pins. Functional fracture stiffness was calculated as

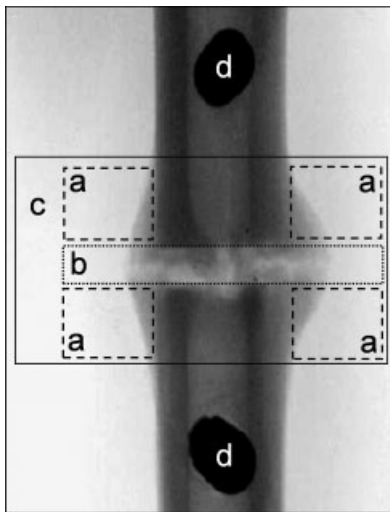


**Figure 2.** Bone mineral content of the healing content was evaluated using DXA, repeatedly positioned through use of the external fixation pins. The three regions of interest included: (a) periosteal intramembranous bone formation (summation of the four regions); (b) interfragmentary endochondral bone formation; and (c) total BMC. The accessory half pins, used to mount the LVDT, are marked by (d), and as seen, are rising out from the figure. The fixator pins are above and below the accessory pins, and are not seen in this image.

the ratio of peak ground reaction force to peak interfragmentary motion. Interfragmentary axial motion at the center of the osteotomy gap was measured, using the assumption of in-plane bending to exclude the effect of bending ( $\pm 2.5 \mu\text{m}^{28}$ ). The average of five strides for each animal were considered at each time point for the analysis.

### Postmortem Mechanical Characteristics

At 10-weeks post-op, the animals were sacrificed by a bolus intravenous injection of pentobarbitone. As an index of restoration of function,<sup>17</sup> healing tibiae from all animals were harvested and tested, for torsional rigidity in a computer-controlled servo hydraulic materials-testing machine with a custom torsion-testing frame, and compared to values from intact tibiae (Dartec, Stourbridge, UK). The least squares linear regression stiffness coefficient and ultimate breaking strength were determined after three low-load preconditioning cycles were applied to the specimen. Pretesting with other ovine fractures indicated a rotational deformation rate of 20 deg/min was optimal for obtaining the most consistent stiffness and low coefficients of variation ( $\text{COV} = 0.031^{15}$ ). All testing was complete within 3 h of euthanasia, saline-soaked

swabs providing cover at all times, and the bones kept at ambient temperature.

### Statistics

All data were pooled by group and analyzed for normality by Lilliefors significance correction for the Kolmogorov–Smirnov test. Normal data were tested for equality of variances between groups (Levene's test) and then the appropriate parametric test applied. Data not normally distributed or not homogeneous were compared using the Mann–Whitney non-parametric comparison of means. Tests were carried out using SPSS for Windows.<sup>29</sup>

## RESULTS

Thirty-Hertz activation of the shape-memory alloy across the fracture site resulted in an initial 25- $\mu\text{m}$  reduction in the space between the two bony ends of the 3-mm osteotomy site (<1% strain of the initial osteotomy gap). One-week post-op, interfragmentary displacement measured during ambulation was similar in both groups, with 0.44 mm in the Experimental group and 0.50 mm in the Controls (Fig. 1;  $p = 0.373$ ), reflecting consistent fracture stabilization and associated mechanical environments. The 30 Hz, 25  $\mu\text{m}$  of interfragmentary displacement induced during stimulation in the Experimental group was less than 6% of that incurred during walking ( $p < 0.001$ ; average of all animals).

### Ground Reaction Forces (GRF)

There were no significant GRF differences between Control and Experimental groups either preoperatively, at baseline, as absolute data or relative data (expressed as a percentage of weekly body weight), emphasizing that there were no functional load-bearing differences between the Control and Experimental groups at any time through the protocol (Student's  $t$ -test,  $p = 0.3807$ ).

### Ambulation and Functional Stiffness

During normal ambulation, the mechanically stimulated fractures had a significantly lower interfragmentary displacement during the 4–6-week period ( $p < 0.05$ ; Fig. 3). Stiffness measured during normal locomotion indicated a trend towards the mechanically stimulated osteotomies regaining stiffness more rapidly by week 5,

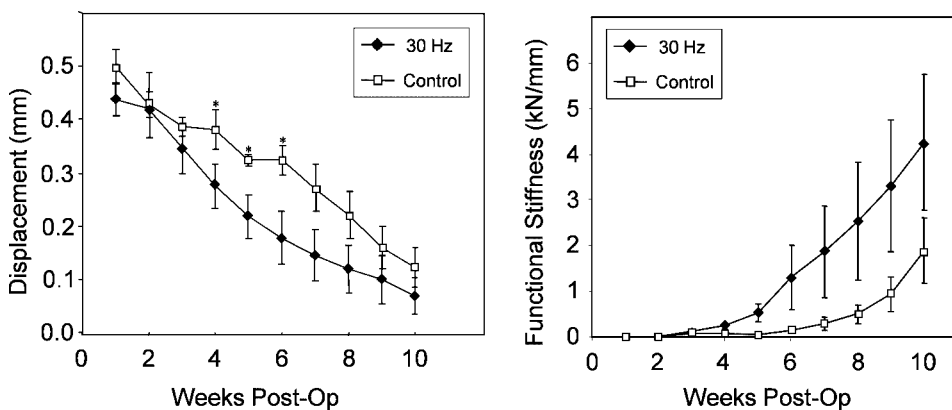


**Figure 3.** Interfragmentary displacement (left) measured by the LVDT during locomotion (mean  $\pm$  SE). As indicated by the asterisk, there are significant differences between the Control (open square) and Experimental (closed diamond) groups at weeks 4, 5, and 6, with the Experimental groups displacing less with weight bearing, but these differences decline by the end of the 10-week protocol. At 10-weeks post-op, functional stiffness (right) measured in vivo during locomotion in the Experimental animals showed no statistically significant difference over Controls ( $p = 0.13$ ).

however, there was no significant difference in functional stiffness after 10 weeks ( $p = 0.13$ ).

### Radiographic Assessment

The blinded radiographic scoring of the rigidly stabilized fractures in the Control animals displayed a range of healing responses graded from no evidence of bridging through to bridging, but not yet remodeling (Table 1). Radiographic assessment in the Experimental group varied from united callus (bridged), through to fully bridged remodeling bony tissue, indicative of an advanced stage of repair (Fig. 4). As measured from the radiographs, the callus diameter of the Control animals ( $19.9 \text{ mm} \pm 2.2$ ) was 22.7% smaller than the callus of the Experimental animals ( $25.7 \text{ mm} \pm 2.6$ ;  $p < 0.01$ ).

### Bone Mineral Content

BMC in the fracture zone of the Experimental animals was 52% higher than Controls (Fig. 5;  $p < 0.02$ ). Further, the proportion of bone in the periosteal regions versus the interfragmentary gap were also significantly different between groups, as the Experimental animals had 262% higher BMC in the periosteal intramembranous regions adjacent to the fracture gap, compared to the Control group ( $p < 0.01$ ), whilst the endochondral bone forming within the interfragmentary region was 32% higher ( $p < 0.05$ ).

### Torsional Rigidity

Examining the biomechanical strength of the fracture site, the regenerate bone in the Experimental group had a 3.6-fold relative increase in torsional stiffness over Control animals (Fig. 6;  $p < 0.03$ ), and a 2.5-fold increase in fracture torsional strength ( $p < 0.02$ ). When compared to the torsional stiffness [ $14.0 \pm 1.9 \text{ Nm}$  (Torque: Newton meters)/degree] and strength ( $69.4 \pm 4.9 \text{ Nm}$ ) of intact tibia, regenerate bone in the Controls was 14% and 10% of intact values, respectively, while the healing fractures in the Experimentals were 64% and 36% of intact tibiae.

## DISCUSSION

Fracture healing is a complex biological process which involves the spatial and temporal orchestration of numerous cell types, hundreds, if not thousands of

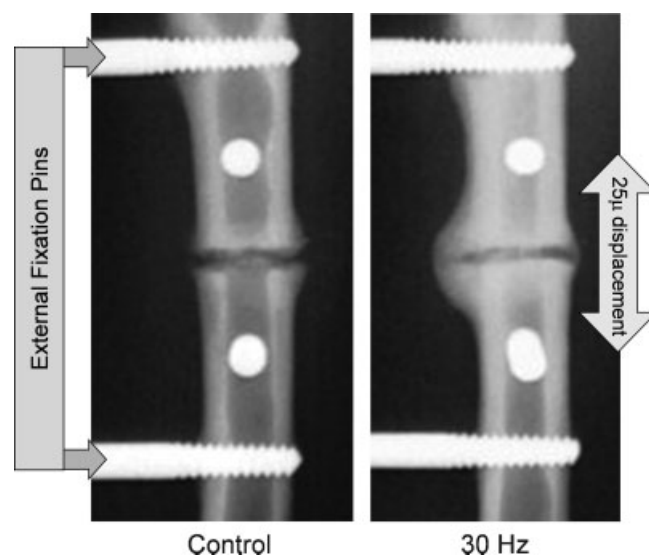


**Figure 4.** Radiographic assessment at 10-weeks post-op of a Control (left) and Experimental (right) animal (contrast controlled using step wedge) showed marked differences between the groups in the size and maturity of the callus (see also Table 1). Also seen on the radiographs are the external fixation pins, and the accessory pins used for mounting the LVDT across the fracture gap. During the active stimulation of the fixator,  $25 \mu\text{m}$  of displacement was induced across the fracture gap. While there is some endochondral bone formation evident in both radiographs at 10 weeks, the extent and maturity of the periosteal callus is much greater on the Experimental animal, contributing to the increased functional stiffness of the fracture gap.

genes, and the intricate organization of matrix, all working towards restoring the bone's mechanical strength and its rapid return to full function.<sup>30</sup> It has often been argued that nature has optimized this process, and thus it would be difficult to interventionally accelerate or augment fracture healing. Nevertheless, when considering the high number of fractures which do not adequately heal,<sup>8</sup> the great efforts to augment and ensure the "correct" healing process through biochemical<sup>31</sup> and biomechanical<sup>32</sup> intervention are certainly justified. Even so, some interventions, such as the use of external or internal fixation devices designed to stabilize the fracture, may also inadvertently compromise the progression of healing through strain protection as a consequence of load sharing between the bone and the device.

In the study reported here, inspired by the potential benefits of weight bearing on fracture healing but

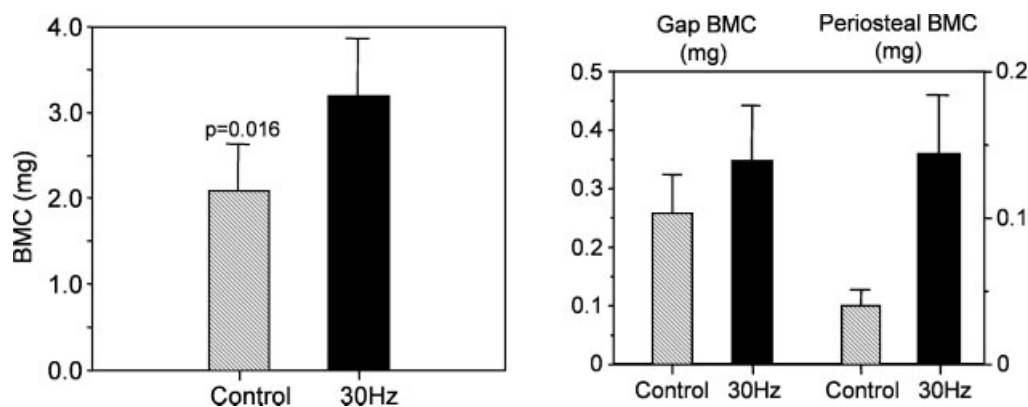


**Figure 5.** As measured by DXA, total callus bone mineral content (left) shows a 52% increase in the total BMC ( $p < 0.02$ ) of the fracture callus in the Experimental animals (Ex) as compared to Controls (Ct). The degree of the healing response in the callus in the Experimental versus Control animals was also site-specific (right), with a 32% increase in the gap BMC ( $p < 0.05$ ) and a 2.6-fold increase in BMC of the periosteal region ( $p < 0.001$ ).

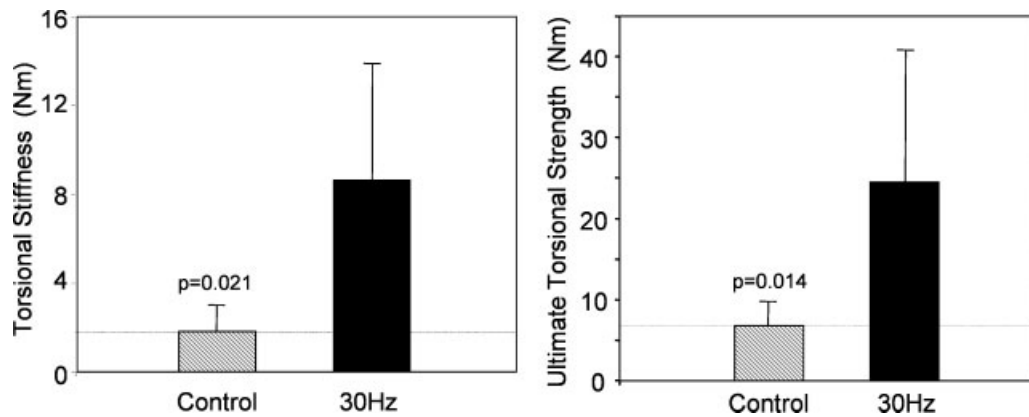


**Figure 6.** Measured at the end of the 10-week protocol, fracture torsional stiffness of the Experimental animals was 3.6-fold higher than Controls ( $p < 0.03$ ). These significant differences were reflected in fracture torsional strength, where the healing fractures in the Experimental animals were 2.5-fold stronger ( $p < 0.02$ ). Relative to the torsional stiffness ( $14.0 \pm 1.9$  Nm/degree) and torsional strength ( $69.4 \pm 4.9$  Nm) of the pooled eight intact tibiae, the 10-week post-op time point showed that the Controls had reached 14% of normal stiffness and 10% of torsional strength, as contrasted to the Experimental animals, which achieved 64% of intact stiffness and 36% of intact strength.

recognizing the risks of overloading the healing tissue,<sup>5</sup> extremely low-magnitude displacements, induced at a relatively high frequency, were used in an attempt to accelerate and augment the healing process. The results from this pilot feasibility trial indicate that these low-amplitude signals, shown to be anabolic to intact bone tissue,<sup>33</sup> can also promote bone repair using displacements applied directly that are well below those induced by functional weight bearing.

This low-magnitude, high-frequency mechanical intervention is based on the premise that there is a physiologic relevance of “other-than-peak” mechanical signals to bone tissue, and that such nonpeak mechanical events represent an important, endogenous regulatory signal in bone remodeling.<sup>34</sup> By examining bone strain data collected from a variety of animals through 12 h over a range of unrestrained activities,<sup>24</sup> including from simple standing (invariably our predominant activity), a broad frequency range of bone strain events is evident. Spectral analysis of these data show that, while there are only a very few ( $< 10$ ), low-frequency, high-magnitude strain events (representing “peak strain magnitudes” of strenuous activity,<sup>24,35</sup> there is also a significant range of mechanical information which, while progressively smaller in amplitude, extends out to beyond 50 cycles per second. Over a period of 12 h, the accumulation of this barrage of mechanical signals which arise from the predominant activities accumulates to hundreds of thousands of extremely small strain events. Thus, in addition to the occasional peak strain events of 2,000 microstrain, very small ( $\ll 5$  microstrain), high-frequency strains persistently bombard the skeleton even during quiet standing.<sup>36</sup>

Considering this power:law relationship in the context of the healing callus, the strain history of intact bone represents “tens” of events arising greater than 1,000 microstrain, hundreds of mechanical events occurring in the range between 50 and 500 microstrain, and tens of thousands of events in the range of 5 to 50 microstrain. Thus, to harness the anabolic potential of mechanical

signals in augmenting and/or accelerating the healing process, it is possible to amplify the mechanical signal delivered by functional demands to the callus by increasing either the large signal component,<sup>9</sup> or as done here, by ramping up the smaller displacements realized in the higher-frequency domain. It is certainly possible that either the “large, low-frequency” or “small, high-frequency” strategies are equally effective in influencing the healing process, but inevitably, the risk of *disrupting* the process by *exceeding* the yield of the fragile regenerate is greater at the higher, rather than the lower, displacements.

In retrospect, it is possible that stabilizing the fracture by either internal or external fixation devices invariably dampen both the large, low-frequency, which arise during function, and the smaller, higher-frequency domain strain signals that originate in muscle contractibility, with the suppression of both contributing to the catabolic consequences of stress shielding. Conversely, reintroducing extremely small interfragmentary motions for 17 min per day, while small relative to the motions generated by walking, are certainly much larger relative to those that arise by muscle activity, and thus serve to augment the anabolic role of mechanical signals without putting the bone—or healing callus—at risk.

High-frequency force components in single motor neuron units increase with load generation up to as high as 40 or 50 Hz in the limb muscles during strong contractions. In nonlocomotory muscles, where fine control is more important than force generation, then these frequencies may extend to over 140 Hz.<sup>37</sup> The majority of motor neurones have a lower-frequency band limit of approximately 11 Hz, even when fatigued, and muscles will either increase force or maintain force output during fatigue by the recruitment of additional neurons.<sup>38</sup> To generate large contractile loads, both the firing frequencies and recruitment of motor neurons increase, which leads to concurrent rises in both mechanical force and the power spectrum of the output frequency. In fractures which are internally or exter-

nally fixed, not only would the “large scale” locomotory stresses and strains on the tissues diminish,<sup>39</sup> but the fixation, itself, would dampen the high-frequency components as a potential regulatory signal to bone. The premise of this intervention is to use a dynamically active fixator to mechanically stimulate the healing tissues without putting the repair process at risk for a short period each day. These exogenously applied, low-amplitude, high-frequency signals applied over a period of only 17 min per day are meant to provide a safe surrogate for the mechanical signals that are typically present in normal loaded intact bone. Given that the displacements which arose during walking far exceeded those generated by the actuator, and the force delivered by the actuator remained a fraction of the weight of the standing animal, we believe that the level of imposed strains would not be detrimental to the tissue differentiation within the callus.

Characteristics of applied micromotion regimens which enhance fracture repair have a physiological basis similar to those which are potent for bone adaptation, emulating frequencies and normal functional loads,<sup>15</sup> but well exceed the strains experienced by the limb during functional activity.<sup>40</sup> This is particularly important, as bone repair comprises two distinct processes of ossification, periosteal intramembranous bone formation followed by interfragmentary endochondral bone formation.<sup>41</sup> Considering that each subsequent tissue is stiffer,<sup>42</sup> the ultimate strain which can be withstood also decreases from very high strains in hematoma and granulation tissue (100%), decreasing to mature bone which can be damaged by as little as 2% strain.<sup>43,44</sup> Hence, as the more advanced tissues form, the integrity of the matrix is much more vulnerable if loads result in motion, displacement, or strain that exceeds the ultimate strain of that particular connective tissue.<sup>2,45</sup>

In this study, the applied load-limited stimulus and resulting displacements, each below those induced by weight bearing, precluded any likelihood that the exogenous mechanical signal would generate damage to the intact or regenerating bone. Additionally, the progression of bridging of callus was seen in both groups as a function of time, further suggesting that physiologic, rather than pathologic processes were involved. A greater callus diameter was evident in the Experimentally stimulated group, resulting in a greater moment of area and associated increased bending strength compared to the nonstimulated Control group.

Although not studied here, once mechanical integrity has been restored, the phase of remodeling that follows can be expected to reduce the callus size and ultimately restore the normal anatomical structure of the bone. We have interpreted the improved torsional stiffness and strength of the Experimental over Control bones to signify a clinical advantage, such that a return to full function and earlier frame removal times would be warranted. This conclusion is supported somewhat by comparing each group to the strength and stiffness values of the intact bone, with the mechanically

stimulated tibiae being significantly closer to reaching these values at 10 weeks than the Controls.

Bone is a tissue that is extremely sensitive to physical signals,<sup>7</sup> but the cellular signals which control the mechanotransduction process are not well known.<sup>46</sup> Not only are physiologically based physical signals central to the proliferation of osteoblasts,<sup>47</sup> they serve to inhibit osteoclastogenesis,<sup>48</sup> and thus represent a key regulatory factor in regulating bone remodeling. It is now evident that physical signals are essential even for the *viability* of bone cells, as bone tissue devoid of stimulation may foster the apoptosis of osteocytes.<sup>49</sup> Of course, the role of mechanical signals extends well beyond bone cells, with clear influences on many cells and tissue types integral to the bone healing process.<sup>50</sup> Indeed, low-magnitude mechanical signals have even been shown to bias the differentiation of mesenchymal stem cells, critical determinants of bone regeneration, towards osteoblastogenesis and away from adipogenesis,<sup>51</sup> inevitably contributing to the augmentation of the healing response.

As we look towards new modalities to treat musculoskeletal injury and disease, bone’s responsivity to mechanical, electrical, and ultrasound signals represent a potent means to influence clinical outcomes. In contrast to biochemical interventions, the attributes of biomechanical-based strategy is that it is native to the bone tissue, safe at low intensities,<sup>27</sup> incorporates all aspects of the remodeling cycle,<sup>48</sup> will ultimately induce lamellar bone,<sup>52</sup> and, depending on the nature of the signal (e.g., load vs. strain), the relative amplitude of the displacement signal will subside as formation persists (self-regulating and self-targeting<sup>53</sup>). However, the widespread use of mechanical—or other physical—stimuli in the treatment of skeletal disorders will undoubtedly be delayed until we achieve a better understanding of the physical and biological mechanisms by which they act.<sup>30,54</sup> The results in this feasibility study suggest that very low levels of displacement, induced through exogenously applied loads, can be used to achieve an enhanced rate and quality of repair. The low levels of displacement in this regimen could be achieved with little risk of mechanical failure of the fixation device and may be applicable to a range of fixation devices.

## ACKNOWLEDGMENTS

The authors are grateful to Bristol University for providing facilities to perform these studies, and to the Benjamin Meaker Professorship which supported C. T. R. during his sabbatical to Bristol University; also to Orthofix srl for providing the fixators and surgical instrumentation, particularly Dr. John Scott for his enthusiastic support. (*Conflicts of Interest:* C. T. R. is a founder of Juvent Medical, Inc., and holds intellectual property that relates to the nature of the mechanical signals described.)

## REFERENCES

1. Claes LE, Wilke HJ, Augat P, et al. 1995. Effect of dynamization on gap healing of diaphyseal fractures under external fixation. *Clin Biomech (Bristol, Avon)* 10:227–234.

2. Gardner TN, Mishra S. 2003. The biomechanical environment of a bone fracture and its influence upon the morphology of healing. *Med Eng Phys* 25:455–464.
3. Augat P, Simon U, Liedert A, et al. 2005. Mechanics and mechano-biology of fracture healing in normal and osteoporotic bone. *Osteoporos Int* 16 (Suppl 2):S36–S43.
4. Chao EY, Aro HT, Lewallen DG, et al. 1989. The effect of rigidity on fracture healing in external fixation. *Clin Orthop* 241:24–35.
5. Augat P, Merk J, Ignatius A, et al. 1996. Early, full weightbearing with flexible fixation delays fracture healing. *Clin Orthop Relat Res* 328:194–202.
6. Goodship AE, Watkins PE, Rigby HS, et al. 1993. The role of fixator frame stiffness in the control of fracture healing. An experimental study. *J Biomech* 26:1027–1035.
7. Wolff J. 1986. *The law of bone remodeling*. Berlin: Springer.
8. Marsh DR, Li G. 1999. The biology of fracture healing: optimising outcome. *Br Med Bull* 55:856–869.
9. Goodship AE, Kenwright J. 1985. The influence of induced micromovement upon the healing of experimental tibial fractures. *J Bone Joint Surg [Br]* 67:650–655.
10. Kenwright J, Richardson JB, Cunningham JL, et al. 1991. Axial movement and tibial fractures. A controlled randomised trial of treatment. *J Bone Joint Surg [Br]* 73:654–659.
11. Carter DR, Blenman PR, Beaupre GS. 1998. Correlations between mechanical stress history and tissue differentiation in initial fracture healing. *J Orthop Res* 6:736–748.
12. Carter DR, Orr TE, Fyhrrie DP, et al. 1987. Influences of mechanical stress on prenatal and postnatal skeletal development. *Clin Orthop* 219:237–250.
13. Huiskes R, Chao EY, Crippen TE. 1985. Parametric analyses of pin-bone stresses in external fracture fixation devices. *J Orthop Res* 3:341–349.
14. Carter DR, Vasu R, Spengler DM, et al. 1981. Stress fields in the unplated and plated canine femur calculated from in vivo strain measurements. *J Biomech* 14:63–70.
15. Goodship AE, Cunningham JL, Kenwright J. 1998. Strain rate and timing of stimulation in mechanical modulation of fracture healing. *Clin Orthop Relat Res* 322(Suppl.):S105–S115.
16. Kenwright J, Goodship AE. 1989. Controlled mechanical stimulation in the treatment of tibial fractures. *Clin Orthop Relat Res* 241:36–47.
17. Richardson JB, Cunningham JL, Goodship AE, et al. 1994. Measuring stiffness can define healing of tibial fractures. *J Bone Joint Surg [Br]* 76:389–394.
18. Aaron R, Bolander M. 2005. *Physical regulation of skeletal repair*. Rosemont, IL: American Academy of Orthopaedic Surgeons.
19. Rubin CT, Lanyon LE. 1985. Regulation of bone mass by mechanical strain magnitude. *Calcif Tissue Int* 37:411–417.
20. Rubin CT, Lanyon LE. 1984. Regulation of bone formation by applied dynamic loads. *J Bone Joint Surg [Am]* 66:397–402.
21. O'Connor JA, Lanyon LE, MacFie H. 1982. The influence of strain rate on adaptive bone remodelling. *J Biomech* 15:767–781.
22. Goodship AE, Lanyon LE, McFie H. 1979. Functional adaptation of bone to increased stress. An experimental study. *J Bone Joint Surg [Am]* 61:539–546.
23. Rubin C, Turner AS, Bain S. 2001. Anabolism: low mechanical signals strengthen long bones. *Nature* 412:603–604.
24. Fritton SP, McLeod KJ, Rubin CT. 2000. Quantifying the strain history of bone: spatial uniformity and self-similarity of low-magnitude strains. *J Biomech* 33:317–325.
25. Carter DR, Caler WE. 1985. A cumulative damage model for bone fracture. *J Orthop Res* 3:84–90.
26. Phillips SJ, Thornton K, Barker L, et al. 1991. Using magnostriptive metal as a pump for biomedical application. *ASAIO Trans* 37:M509–M510.
27. Carter DR, Caler WE, Spengler DM, et al. 1981. Fatigue behavior of adult cortical bone: the influence of mean strain and strain range. *Acta Orthop Scand* 52:481–490.
28. Lawes TJ, Scott JC, Goodship AE. 2004. Increased insertion torque delays pin-bone interface loosening in external fixation with tapered bone screws. *J Orthop Trauma* 18:617–622.
29. Zar JH. 1996. *Biostatistical analysis*. Upper Saddle River, NJ: Prentice Hall.
30. Hadjiargyrou M, Lombardo F, Zhao S, et al. 2002. Transcriptional profiling of bone regeneration: insight into the molecular complexity of wound repair. *J Biol Chem*. 277:30177–30182.
31. Wozney JM, Rosen V. 1998. Bone morphogenetic protein and bone morphogenetic protein gene family in bone formation and repair. *Clin Orthop* 346:26–37.
32. Heckman JD, Ryaby JP, McCabe J, et al. 1994. Acceleration of tibial fracture-healing by non-invasive, low-intensity pulsed ultrasound. *J Bone Joint Surg [Am]* 76:26–34.
33. Rubin C, Turner AS, Muller R, et al. 2002. Quantity and quality of trabecular bone in the femur are enhanced by a strongly anabolic, noninvasive mechanical intervention. *J Bone Miner Res* 17:349–357.
34. Rubin CT, Sommerfeldt DW, Judex S, et al. 2001. Inhibition of osteopenia by low magnitude, high-frequency mechanical stimuli. *Drug Discov Today* 6:848–858.
35. Adams DJ, Spirt AA, Brown TD, et al. 1997. Testing the daily stress stimulus theory of bone adaptation with natural and experimentally controlled strain histories. *J Biomech* 30:671–678.
36. Huang RP, Rubin CT, McLeod KJ. 1999. Changes in postural muscle dynamics as a function of age. *J Gerontol A Biol Sci Med Sci* 54:B352–B357.
37. Clamann HP. 1969. Statistical analysis of motor unit firing patterns in a human skeletal muscle. *Biophys J* 9:1233–1251.
38. Person RS, Kudina LP. 1972. Discharge frequency and discharge pattern of human motor units during voluntary contraction of muscle. *Electroencephalogr Clin Neurophysiol* 32:471–483.
39. Carter DR, Vasu R. 1981. Plate and bone stresses for single- and double-plated femoral fractures. *J Biomech* 14:55–62.
40. Rubin CT, Lanyon LE. 1982. Limb mechanics as a function of speed and gait: a study of functional strains in the radius and tibia of horse and dog. *J Exp Biol* 101:187–211.
41. Brunelli MP, Einhorn TA. 1998. Medical management of osteoporosis. *Fracture prevention*. *Clin Orthop* 348:15–21.
42. Augat P, Margevicius K, Simon J, et al. 1998. Local tissue properties in bone healing: influence of size and stability of the osteotomy gap. *J Orthop Res* 16:475–481.
43. Augat P, Reeb H, Claes LE. 1996. Prediction of fracture load at different skeletal sites by geometric properties of the cortical shell. *J Bone Miner Res* 11:1356–1363.
44. Kelly PJ, An KN, Chao EYS, et al. 1985. Fracture healing: biomechanical, fluid dynamic and electrical considerations. In: Peck WA, editor. *Bone mineral research*. New York: Elsevier. p 295–319.
45. Claes L, Eckert-Hubner K, Augat P. 2003. The fracture gap size influences the local vascularization and tissue differentiation in callus healing. *Langenbecks Arch Surg* 388:316–322.
46. Rubin J, Rubin C, Jacobs CR. 2006. Molecular pathways mediating mechanical signaling in bone. *Gene* 367:1–16.
47. Burger EH, Klein-Nulen J. 1999. Responses of bone cells to biomechanical forces in vitro. *Adv Dent Res* 13:93–98.



48. Rubin J, Fan X, Biskobing DM, et al. 1999. Osteoclastogenesis is repressed by mechanical strain in an in vitro model. *J Orthop Res* 17:639–645.
49. Noble BS, Peet N, Stevens HY, et al. 2003. Mechanical loading: biphasic osteocyte survival and targeting of osteoclasts for bone destruction in rat cortical bone. *Am J Physiol Cell Physiol* 284:C934–C943.
50. Einhorn TA. 1996. Enhancement of fracture healing. *Instr Course Lect* 45:401–416.
51. Rubin CT, Capilla E, Luu YK, et al. 2007. Adipogenesis is inhibited by brief, daily exposure to high-frequency, extremely low-magnitude mechanical signals. *Proc Natl Acad Sci USA* 104:17879–17884.
52. Rubin CT, Gross TS, McLeod KJ, et al. 1995. Morphologic stages in lamellar bone formation stimulated by a potent mechanical stimulus. *J Bone Miner Res* 10:488–495.
53. Judex S, Boyd SK, Qin YX, et al. 2003. Adaptations of trabecular bone to low magnitude vibrations result in more uniform stress and strain under load. *Ann Biomed Eng* 31:12–20.
54. Rubin J, Rubin CT, McLeod KJ. 1995. Biophysical modulation of cell and tissue structure and function. *Crit Rev Eukaryot Gene Expr* 5:177–191.